American Journal of Physics and Applications
2014; 2(6): 135-144
Published online December 16, 2014 (http://www.sciencepublishinggroup.com/j/ajpa)
doi: 10.11648/j.ajpa.20140206.14
ISSN: 2330-4286 (Print); ISSN: 2330-4308 (Online)

Acoustical phonons transport through a stepped quantum wire

Mohammed Saïd Rabia

Laboratoire de Mécanique des Structures et Energétique, Université Mouloud Mammeri, BP 17 RP Hasnaoua II, Tizi-Ouzou 15000, Algérie

Email address:
m2msr@yahoo.fr

To cite this article:
Mohammed Saïd Rabia. Acoustical Phonons Transport through a Stepped Quantum Wire. *American Journal of Physics and Applications.* Vol. 2, No. 6, 2014, pp. 135-144. doi: 10.11648/j.ajpa.20140206.14

Abstract: This work presents a theoretical approach for the study of phonon dynamics and scattering properties of an infinite linear atomic chain perturbed by a mono atomic step. The coherent transmittance scattering cross-sections for incident phonons on the atomic waveguide structure are calculated using the Landauer-Buttiker electron scattering description and the matching method formalism with the nearest and next nearest neighbour interactions. Numerical results for different configurations yield an understanding of the chain dynamical properties and the effects on phonon transmittance due to incoming phonons. The reflectance and transmittance coefficients show spectral characteristic features depending on the cut-off frequencies for the propagating phonons. They illustrate the occurrence of Fano resonances in the scattering spectra that result from degeneracy of step localized modes and propagating continuum modes due to the breakdown of the translation symmetry in the propagating direction. Furthermore, the interferences between diffused and reflected waves in the step regions generate Fabry-Pérot oscillations whose number is determined by the distance between steps and the number of terraces.

Keywords: Reticular Dynamics, Disordered Mesoscopic Systems, Crystallographic Waveguides, Matching Procedure, Phonon Scattering

1. Introduction

The presence of reticular defects in a structure affects substantially its dynamic, thermodynamic and kinetic properties. To study this influence, we must elucidate the phonons-defect interaction problem [1-5]. Interference effects generated in the elastic waves scattering by the reticular defects found a considerable interest since they can give rise to the resonant features of inter-crystalline interfaces which can be observed experimentally. Several authors [6–12] have shown that multiple scattering occupies a privileged place in the description of the transport phenomena. This point of view acquired these last years a certain practical importance owing to advances in nanotechnologies [13–17]. Indeed, it allows a better understanding in what occurs in low-dimensional compounds such as quantum wires [8-9,18-19]. In this sense, scattering experiments are undertaken in various fields of physics in order to study the properties of mesoscopic systems.

The modern developments of the lattice dynamics theory and its many applications have been discussed in detail in standard references such as Born and Huang [20], Lubfried and Ludwig [21], Maradudin and *al.* [23]. However, this theory of big convenient range concerns only the infinite systems. Large amounts of calculations, relating phonons in semi-infinite crystals are essentially based on the Green functions methods [15,22]. The matching method [6-8], derived from the Landauer-Büttiker principle [2,3], to which we resort makes it possible to analyze the behaviour of the elastic waves through the defect perturbed region. We are interested, in particular, with the effects produced by this interaction on the phonons transmittance spectrum within the long-wave limit and low-frequency [1,7,8]. The results obtained for the 1D model [9] coincide with that obtained for 3D one [24] with the precision up to the numerical factor. In this work, however, we consider the propagation and the diffusion of the phonons by the structural defect in a 1D atomic chain. In spite of their simplicity, the one dimensional models give a qualitative description of many physical phenomena observed in the real three-dimensional systems.

The organization of this paper is as follows. In Section 2, we present the basic elements of model. Section 3 describes briefly the numerical method formalism. The numerical results for an isolated step and multiple steps are discussed in

Section 4. Finally, a summary is made in Section 5.

2. Description of the Model

The considered model depicted in Fig. 1, is made of an infinite atomic nanowire assimilated to a perfect quantum waveguide, so as to form an isolated step according to the y direction. The mono-atomic step (defect region indicated by the grey area *M*) is treated as the perturbed interface between two single semi infinite atomic nanowires *G* (left) and *D* (right) occupying the half spaces on either side of the step. The implied interactions refer only to the bonding strengths between nearest and next nearest close neighbours. The bonding force between two close atoms of the nanowire is symbolized by a spring constant k_1; the other additional constants as k_{lv1} and k_{lv2}, are represented on the figure. There is experimental evidence that the frequencies of the localized vibrational states on the step can be either greater than the maximum frequency of the bulk phonon spectrum [26], or smaller than the frequency of the surface phonon mode [27] of the terraces. This has been modelled by attributing stiffened [28] or loosened [27] force constants in the neighbourhood of the step.

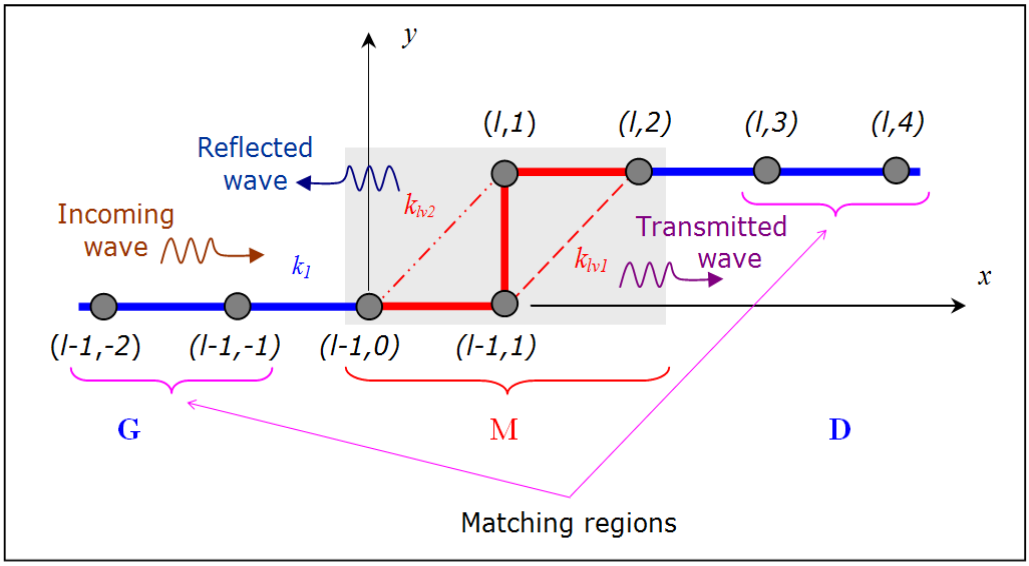

Figure 1. *Schematic representation of a 1D waveguide. The mono-atomic step is treated as the perturbed interface (grey area M) between two single semi infinite atomic nanowires G and D.*

3. Matching Method Principle

Initiated by Feuchtwang in the sixties then revisited by Szeftel and *al.* in the eighties, the matching method returns account in a satisfactory way for the phonons dispersion curves [7] and for surface resonances. It gives also a more general definition of the resonance concept and allows a more transparent analysis of the displacements behaviour in the vicinity of the Van Hove singularities [29]. However, its execution requires the crystal subdivision in three distinct regions having all the same periodicity along the surface. The procedure was described in details in references [7-9]. We will just present the necessary stages to the comprehension of the results analysis.

3.1. Perfect Nanowire Dynamics

For an atom occupying the site (*l*) confounded with the origin of the coordinates system and vibrating at the frequency ω, the equations of motion can be written, using the harmonic approximation framework [23], in the following form:

$$\omega^2 m(l) u_x(l) = -k_1(u_x(l) - u_{x+1}(l')) - k_1(u_x(l) - u_{x-1}(l')) \quad (1)$$

where m indicates the atom mass; u_x the atomic displacement and k_1 symbolises the bonding strength constant between the two adjacent atoms localized at sites *(l)* and *(l')*.

Taking into account the symmetry of the problem [30] and while applying the scattering boundary conditions for which we get plane wave solutions, the perfect lattice atom equation of motion (1) rewrites itself in following form:

$$\Omega^2 - 2 + (Z + 1/Z) = 0\,, \quad (2)$$

where $\Omega = \sqrt{m\omega^2/k_1}$ is the dimensionless frequency and Z the phase factor of the plane wave.

For $Z = e^{iqa}$, the resolution of the equation (2) determines the eigenfrequencies Ω as well as the corresponding eigenvector $\vec{u}_x$. When the real wavevector q is running over the first Brillouin zone, one obtains the dispersion curve $\Omega(q)$. Fig. 2 shows the shape of this curve, symmetrical relatively to frequency axis in the case of a lattice

parameter $a=1$, $k_1=1$ and $m=1$.

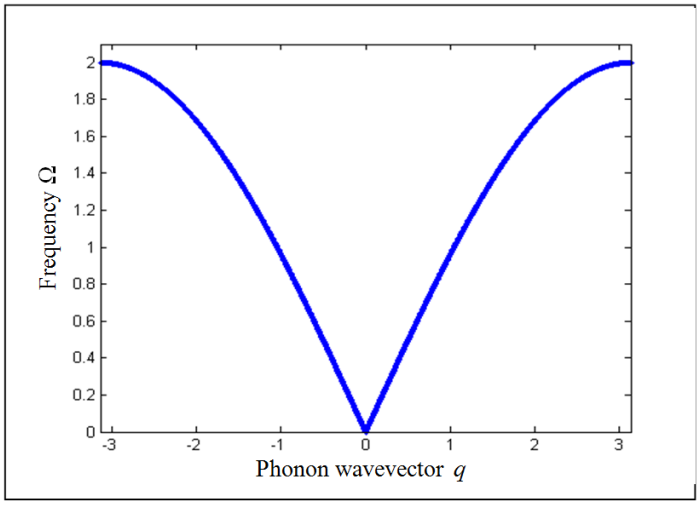

Figure 2. *Dispersion branch of the propagating mode characterizing the perfect atomic nanowire.*

Contrary to the electronic case where the curves are parallel sinusoids, we do not have here any hope to find a usable analytical expression. It will thus be necessary to resort to purely numerical methods to integrate this dispersion relation in the general problem in presence of defect. The result indicates that the only chain mode of vibration is acoustic ($\Omega \to 0$ as $q \to 0$).

The treatment of the scattering problem in presence of defects imposes the simultaneous knowledge of the propagating part ($|Z|=1$) defined previously and the evanescent one ($|Z|<1$) of the perfect 1D waveguide. In other words, for a given frequency, all solutions are necessary even those whose module is lower than unity. The solution which can be obtained by inversing the dispersion relation yields the functional behaviour of the vibrating eigenmode shown in Fig. 3. The projection of the curves on the complex Z plan shows that propagating mode solution follows the circle of unity radius equal to the module of the phase factor Z; this solution is identified to the dispersion curve of Fig. 2. The evanescent solution ($|Z|<1$), beyond the maximum frequency in this branch, corresponds to the curve contained inside the unit circle.

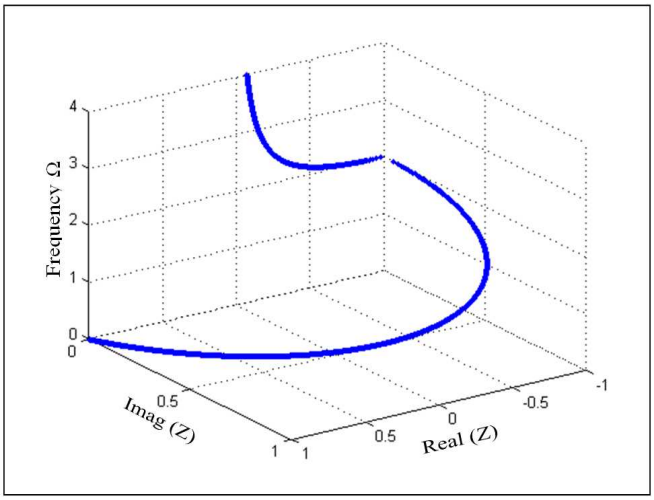

Figure 3. *Functional behaviour* $\Omega(Z)$ *of the vibrating mode of the perfect lattice quantum wire*

3.2. Coherent Phonons Scattering at the Step Edge

Since the perfect waveguides do not couple between different eigenmodes, we can treat the scattering problem for each vibratory eigenmode separately. Generalization to every combination of these modes does not pose a particular problem. For an incidental wave V_{in} coming from the left of figure 1 in the eigenmode ν,

$$\vec{V}_{in}^{\,i} = (Z)^{\,i}\,\vec{u}\,, \tag{3}$$

where Z is the phase factor of the entering mode, $\vec{u}$ its eigenvector. The superscript $i\,(\leq -1)$ indicates the site occupied by the atom relatively to the direction of

propagation.

The resulting scattered waves, due to an elastic scattering by the defect, are composed of reflected and transmitted parts which generate vibrational fields in the two unperturbed half spaces G and D (Fig.1). The Cartesian displacement components of an atom pertaining to these areas can be obtained by using the matching method [7]. For such a site, the displacement components are expressed as a superposition of the perfect waveguide eigenmodes at the same frequency, i.e.:

$$\vec{u}_r^{\,i} = \xi . \left[\frac{1}{Z}\right]^i . \vec{u}\left(\frac{1}{Z}\right), \quad i \le (l-1,-1), \tag{4}$$

$$\vec{u}_t^{\,i} = \eta . \left[Z\right]^i . \vec{u}\left(Z\right), \quad i \ge (l,3), \tag{5}$$

where ξ and η indicate the reflection and transmission probabilities. The normalization of these coefficients with respect to the group velocity (shown in Fig. 4) of the plane wave gives transmittance $\Lambda = \eta / Vg$ and reflectance $\chi = \xi / Vg$. In this case, we obtain unitarity of the scattering matrix.

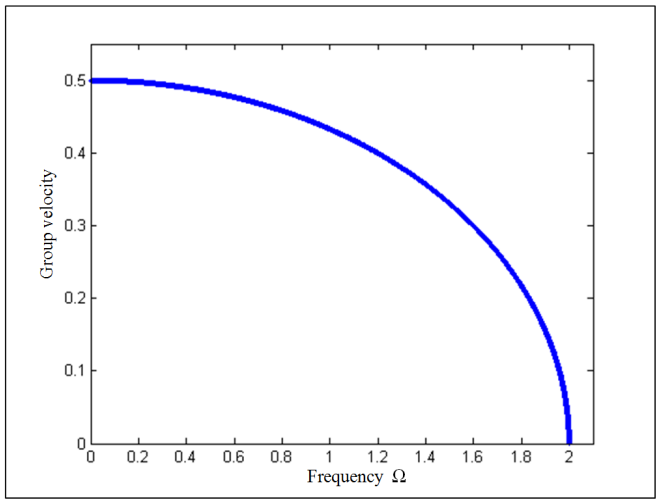

Figure 4. *Phonon group velocity of the perfect atomic chain as function of the dimensionless frequency.*

By isolating the terms describing the incidental wave by using the relations (4) and (5), the inhomogeneous system of linear equations is finally put in the form:

$$\left[\tilde{D}(\Omega, k_l, k_{lv1}, k_{lv2})\right][R]\vec{X} = -\left[\tilde{D}(\Omega, k_l, k_{lv1}, k_{lv2})\right]\vec{V}_{in}, \tag{6}$$

where $\left[\tilde{D}(\Omega, k_{lv1}, k_{lv2})\right]$ represents the dynamical matrix of the defect, $\vec{V}_{in}$ the incidental vector and $\vec{X}$ the vector gathering all the problem unknowns: the atomic displacements u_x of the defect atoms as well as the reflectance and the transmittance coefficients. These are necessary for the determination of atomic displacements in the boundaries as in the unperturbed areas *G* and *D* of the perfect waveguide.

As example, for the isolated step of Fig. 1 we obtain a dynamical matrix $\tilde{D}\left[6\times 8\right]$ from where a matching matrix $R\left[8\times 6\right]$ is deduced. Then the vector $\vec{X}$ will be composed of six unknowns including the four vibrational displacements $u_x(l)$ of the step irreducible atoms and two transmittance and reflectance probabilities, *i.e.*

$$\vec{X} = \left\{u_x(l-1,0),\ u_x(l-1,1),\ u_x(l,1), u_x(l,2),\ \chi, \Lambda\right\}$$

3.3. Phonons Spectra of Irreducible Step Atoms

In combining the matching procedure to the Green's functions and for a given wave vector parallel to the direction of propagation, the matrix phonon spectral density reads

$$\rho^{(l,l')}_{(\alpha,\beta)}(\Omega) = -2\Omega \sum_m P^l_{\alpha i} P^{l'}_{\beta i} \delta(\Omega^2 - \Omega_m^2), \tag{7}$$

where (*l*) ands (*l'*) are two atomic sites, α and β designate two different Cartesian directions and $P^l_{\alpha i}$ is the component in direction α of the polarization vector of the atom (*l*) for the mode having a frequency Ω_m.

The vibration density of states (DOS) $N_i(\Omega)$ per atomic site in the perturbed defect region could be calculated by summing over the trace of the spectral density matrix ($G(\Omega^2 + j\varepsilon) = ((\Omega^2 + j\varepsilon)I - D_f(r_2, \lambda))^{-1}$ being the Green operator), i. e for $(l) = (l')$,

$$N_l(\Omega) = -\frac{2\Omega}{\pi} \lim_{\varepsilon \to 0^+} \left\{ \sum_\alpha \mathrm{Im}\left[G^{ll}_{\alpha\alpha}(\Omega^2 + j\varepsilon)\right] \right\} \tag{8}$$

4. Numerical Results and Discussion

4.1. Scattering at the Single Surface Step

Phonons scattered by the step are analyzed relatively to an incident wave coming from the left in Fig. 1, with unit amplitude and a zero phase on the border atom (-1) located just at the site near the defect region *M*. Calculation is carried

out for $k_1 = 1$, $k_{lv1} = 1.2$ and $k_{lv2} = 0.8$. The numerical results obtained for the transmittance and reflectance probabilities in terms of the normalized dimensionless frequency are consigned in Fig. 5.

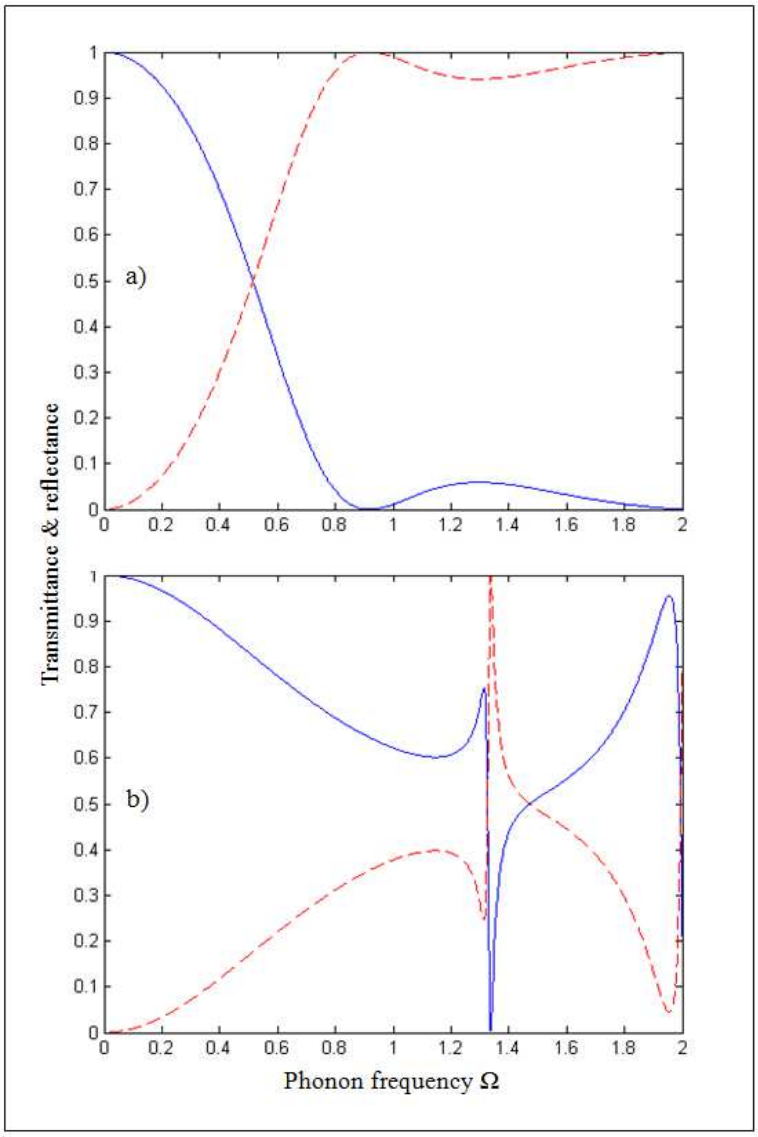

Figure 5. *Phonon transmittance Λ (full line) and reflectance χ (dotted line) as a function of scattering frequency for an isolated monatomic step in the case of a) loosened and b) stiffened force constants in the neighbourhood of the step.*

We notice that the presence of the step leads to a general decrease of the probability. As expected, the influence of the defect is relatively small in the acoustical regime because of the low implied frequencies. For $\Omega \to 0$ we get $\Lambda \to 0$ in addition to the pronounced typical Fano-like resonance structure. This asymmetric resonance can be attributed to the presence of defect-induced resonant state, whose frequency depends on the value of the bonding forces in the step region.

This generalized behaviour is also observed when backscattering becomes more significant for wave vectors near the zone boundary where the transmittance probability tend towards zero. Lastly the well known theoretical relation translating the conservation of energy principle,

$$\left(|\Lambda| + |\chi|\right) = 1, \tag{9}$$

is fortunately satisfied and always checked for each frequency. Besides, this condition constitutes an effective control method of the results.

Otherwise the spectrum is much more affected in the case of loosened force constants. In addition to resonance, this influence is translated by a less amplitude compared to the stiffened constants values.

4.2. Isolated Double Step

The surface-surface phonon scattering is now considered for a double step, schematized in top of Fig. 6, where the two step edges are sufficiently far apart to justify decoupling the dynamics of the two edges. However, there exists a domain where the two edges are still sufficiently close (δ corresponds to a distance smaller than the surface phonon coherent length) where the two steps interact by exchanging

coherent surface phonons.

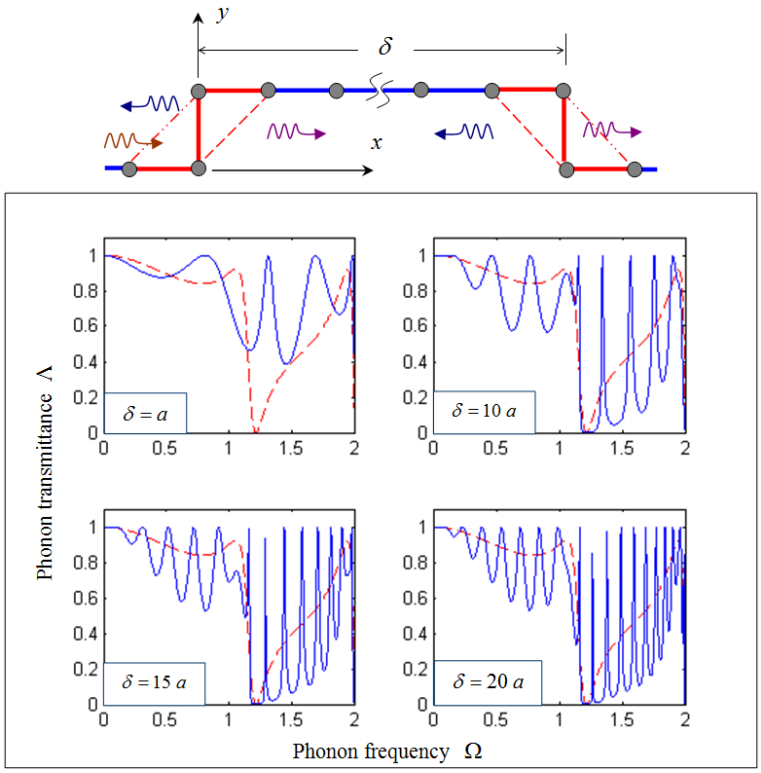

Figure 6. *Magnitude of the phonon transmittance as function of the scattering frequency for two identical steps separated by a distance* δ *in the case of loosened force constants in the neighbourhood of the step. The dotted line refers to single step with the same parameters. The structure scheme is given above the figure.*

Fig. 6 gives the example of two identical steps separated by a plateau of variable length δ and the transmittance probabilities they produce.

The effects described previously in the case of isolated step appear, but they are even more difficult to isolate because of the biggest number of peak-dip structures near in frequencies. It is why we are not going to study in details these regions. On the other hand, we will limit ourselves to present a more global change of the transmission curves, provoked by the Fabry-Pérot oscillations issued from interferences between the multiple scatterings of propagating states in the perturbed region.

The distance δ represents always a whole multiple of network parameters a. It can be seen in Fig. 6 that the transmittance curves structure became richer of several peaks. We observe also a drastic δ dependence of Fabry-Pérot oscillations. However, the number of main dips remained the same corresponding to the number of steps; but each of them divides in several secondary peaks that provide the total number of lattice parameter a contained in horizontal distance δ.

The fact that their number seems to be lower on the figure is simply related to a resolution problem in the implied frequency range. Same results are observed by V. Pouthier and *al*. [18] on the transmittance spectrum of a nanowire containing a set of linear clusters separated by different spacings. Some rapid oscillations in the boundary are due to the simultaneous presence of Fabry Pérot interferences which become more and more important with the increase of δ. The transmission spectrum displays more complex oscillation behaviours especially for higher frequency. Otherwise, the upper level of the Fabry Pérot oscillation can merge with the Fano-resonance peak. It should be noted that on average the global shape of the transmission curves is quite similar to that obtained in the case of an isolated step (in dotted line on the figure).

4.3. Interaction of Several Steps

The increase of the sample defect region doesn't bring anything of qualitatively new in relation to the case of the isolated step. The addition of steps results solely in the increase of the size of the linear system (6), but the matrix $\tilde{D}$ keeps its structure. The supplementary blocks have the same shape as those characterizing a lonely isolated step. Naturally, we can be interested by a disposition of consecutive steps forming a staircase. We have limited our study to only fifteen steps which already generates a (34×36) defect matrix dimension. In Figs. 7 and 8, we investigate the dependence of the transmittance probabilities as function of the dimensionless frequency for different staircases in both cases of stiffened (Fig. 7) and loosened (Fig. 8) force constants in the perturbed step region. The dotted lines refer to a single isolated step. The transmission curves are turned into a number of peak-dip structures, the reason is that the modes will interfere with each other due to the multiple reflections

of the phonon waves in the perturbed region. In general, the multiple interferences in the perturbed waveguide imply the more complex transmittance spectra, especially for higher (Fig. 7) and lower (Fig. 8) frequencies. These interferences between multiply scattered waves result in Fabry–Pérot oscillations of increasing amplitudes with the frequency and whose number depends intimately of the number *N* of steps that the staircase includes. Similar results are obtained in the study of adatomic defects [9,12,31-32] and substitutional defect columns [8] in the perturbed double quantum chain. Defects are separated by different spacings in both configurations.

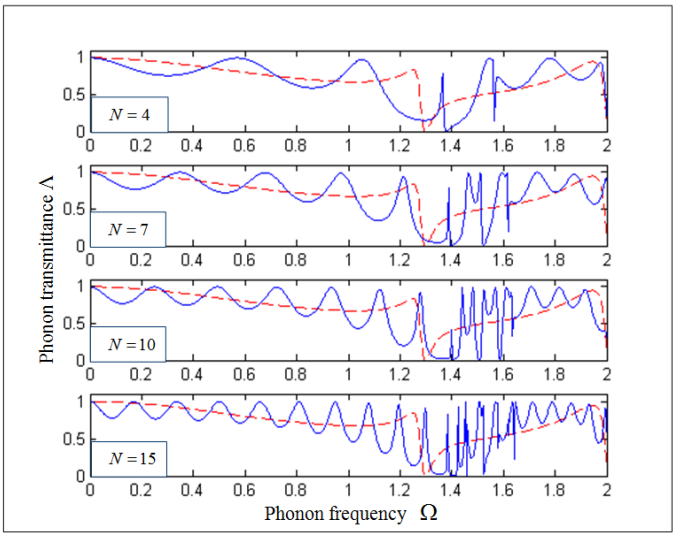

Figure 7. *Phonon transmittance versus scattering frequency for staircase having a variable number N of steps in the case of stiffened force constants in the perturbed step region. The dotted line refers to single step for the same parameters.*

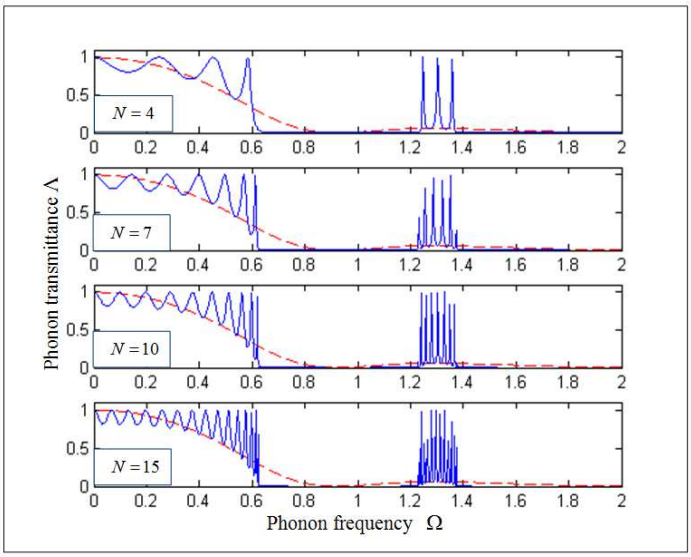

Figure 8. *Phonon transmittance versus scattering frequency for staircase having a variable number N of steps in the case of loosened force constants in the perturbed step region. The dotted line refers to single step for the same parameters.*

An interesting feature is that the dips which correspond to positions of transmission zero, shown in the middle frequency interval broaden with the increase of the step number and develop gradually into a stop frequency gap at which all phonons are reflected by the defect quantum waveguide. Note that on average, the transmission curves follow a shape globally similar to that of the isolated step in both states of strengths in a step region.

4.4. Distributed Terraces

Figs. 9a) to 9d) show some examples of regular sets of terraces and the corresponding transmittance coefficients that they produce in the acoustical mode of the linear quantum waveguide. As previously, the dotted curves refer to an isolated step. The transmittance spectra present qualitatively the same behaviour. In relation to the case of the isolated step, the structure of the transmittance curves became richer of several peaks. However, the number of main peaks remained the same, giving the distance between two consecutive steps; but each of them is subdivided in several secondary peaks that provide the total number of terraces of the structure. Same results are observed by V. Pouthier and *al*. [18] on the

transmittance spectrum of set of clusters separated by different spacings in a nanowire and by Fellay and *al*. [27] on the transmission probability for a sequence of equidistant symmetric local mass defects. We also observed the same spectral behaviour in studying the transmission coefficient of adatomic sequences in the planar quantum waveguide [28] and in the double quantum chain [30].

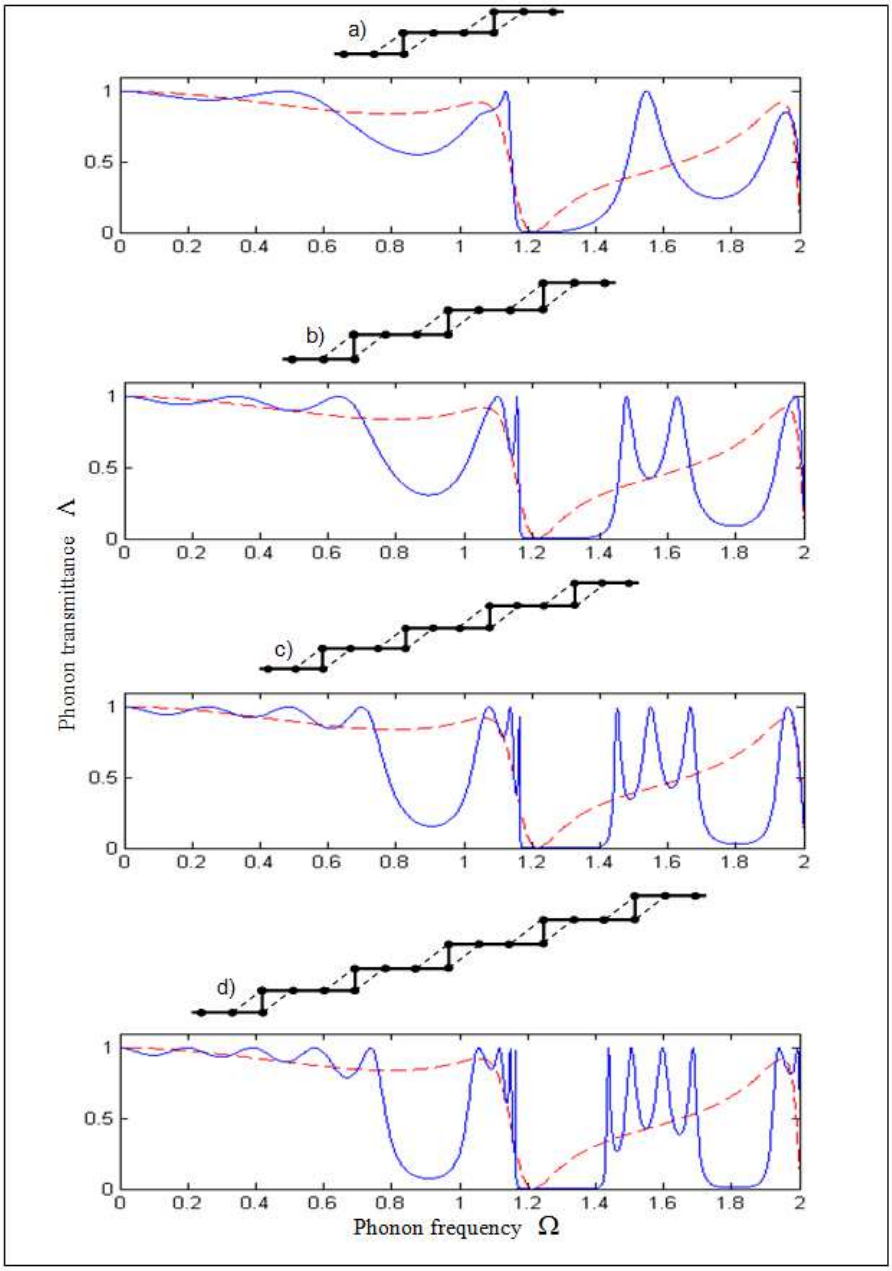

Figure 9. *Phonon transmittance probabilities versus scattering frequency for a structure having a defect composed of one (a), two (b) three (c) and four (d) terraces of the same dimension. The dotted curve refers to single isolated step. The structure scheme is given above each figure.*

One can find from the figure that an additional terrace structure makes the frequency gap appear; and the gap width increases slightly with the step number. Furthermore, it is obviously that the width of resonance peaks at the frequency just near the gap region decreases. We can easily expect that an additional terrace structure increases the scattering of the phonons so that the thermal conductivity decreases.

4.5. Phonons Densities of States

In Fig. 10 we show the phonon densities of states (DOS) versus the normalized frequency for the set of the irreducible atoms (a), (b) and (d) of the perturbed mono-atomic step region M (see Fig. 1).

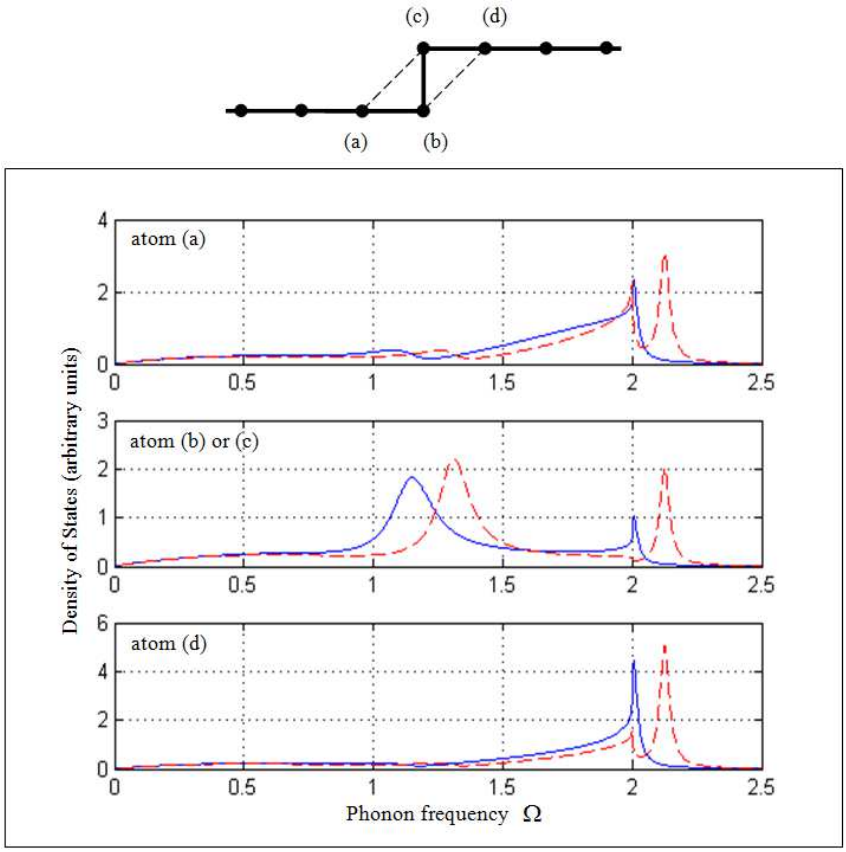

Figure 10. *Density of states vs. incident phonon frequency for irreducible atoms of the mono-atomic step.*

The results were calculated, according to Eq. (8), in the cases of loosened ($k_{lv1}=1.2$ and $k_{lv2}=0.8$, full line) and stiffened ($k_{lv1}=1.6$ and $k_{lv2}=1.2$, dotted line) force constants in the neighbourhood of the step. Due to obvious symmetry effects, quite similar behaviors are observed for the couple of step atoms (b) and (c) above of Fig. 10. The both atoms (a) and (d), on both sides of the step, present the spectral curves with different amplitudes. It can be seen that DOS spectra of the irreducible step atoms are all characterized by two resonant peaks in the case of stiffened force constants. However, there is one common resonant state. This high-frequency peak occurring always at $\Omega=2.0$ corresponds mainly to the longitudinal atomic chain mode near the Brillouin zone boundaries. On all sides, the other resonant peak shifts to higher frequencies with the force constants values according to the relation $\Omega=\sqrt{k/m}$. This phonon localized mode is due to the presence of the mono-atomic step.

5. Conclusion

Using the matching method formalism, we have investigated the phonon transmission in a linear waveguide nanostructure perturbed by a mono atomic step as reticular defect. It is observed strong resonant transmission determined by phonon scattering in step region. The position and the width of the resonance peaks are determined by loosened or stiffened force constants in the neighbourhood of the step.

The transmittance coefficients in multiple step structures are also studied. The results show that the first additional step to the single step structure induces interferences which become more and more important with the increase of the plateau width δ. However, the number of main dips corresponds to the number of steps; but each of them divides in several secondary peaks that provide the total number of lattice parameter a contained in δ. The transmittance spectra present qualitatively the same behaviour in considering several steps or terraces. An additional step structure suppresses the transmittance coefficient and forms a frequency gap; an additional resonance peak appears at the frequency just above the gap region for each additional step structure. The additional step structure increases the phonons scattering so that the thermal conductivity decreases.

References

[1] B. Kramer, *Quantum Coherence in Mesoscopic Systems*, (plenum, New York, 1991).

[2] E. Tekman and P. F. Bagwell, *Phys. Rev*. B48 (1993) 18 299.

[3] Yu A. Kosevich, *Prog. Surf. Sci*. vol 55 (1997) 1.

[4] R. Landauer, *Z. Phys.* B 68 (1987) 217; *J. Phys. Condens. Matter* 1 (1989) 8099.

[5] M. Büttiker, *Phys. Rev. Lett*. 57 (1986) 1761.

[6] E. S. Syrkin, P.A. Minaev, A. G. Shkorbatov and A. Feher, *Microelec. Eng.* vol. 81, (2005) 503.

[7] J. Szeftel and A. Khater, *J. Phys C* 20 (1987) 4725.

[8] A. Fellay, F. Gagel, K. Maschke, A. Virlouvet and A. Khater, *Phys.Rev*. B 55 (1997) 1707.

[9] M. S. Rabia, *J. Mol. Struc-Theochem* 777 (2006) 131-138.

[10] A. Khater, N. Auby and D. Kechrakos, *J. Phys. Condens. Matter* 4 (1992) 3743-3752.

[11] C. Berthold, F. Gagel and K. Maschke, *Phys. Rev.* B 50 (1994) 18299.

[12] F. Gagel and K. Maschke, *Phys. Rev.* B 52 (1995) 2013.

[13] H. Ibach and D. L. Mills, *Electron Energy Loss Spectroscopy and Surface Vibrations,* (New York: Academic, 1982)

[14] P. F. Bagwell, *Phys. Rev.* B 41 (1990) 10354; *J. Phys. Condens. Matter* 2 (1993) 6179.

[15] R. E. Allen, G. P. Alldrege and F. W. Wette, *Phys. Rev.* B 4 (1971) 1648.

[16] P. Knipp, *Phys. Rev.* B 43 6908 (1991).

[17] G. M. Watson, D. Gibbs and D. M. Zehner, *Phys. Rev. Lett.* 71 (1954) 3166.

[18] V. Pouthier and C. Girardet, *Phys. Rev.* B 66 (2002) 115322.

[19] M. S. Rabia, 10ème *Congrès Français d'Acoustique*, Lyon (2010), France.

[20] M. Born and K. Huang, *Dynamical Theory and Crystal Lattices* (Oxford University Press, New York, 1954).

[21] G. Lubfried and W. Ludwig, *Solid State Physics*, vol. 12 edited by F. Seitz and Turnbull (Academic Press Inc., New York, 1961).

[22] L. M. Lifshitz and L. N. Rosenzweig, *Ekperim. Theor. Fiz*. 18 (1948) 1012.

[23] Maradudin A. A., Montroll E. W., Weiss G. H. and Ipatova, *Theory of lattice Dynamic in the Harmonic Approximation,* Academic Press New York and London (1971).

[24] M. S. Rabia, H. Aouchiche and O. Lamrous, *Eur. Phys. J. – A. P.* 23 (2003) 95-102.

[25] M. S. Rabia, *J. Phys. Condens. Matter* 20 (2008) 465218.

[26] H. Ibach and D. Bruchmann, *Phys. Rev. Lett.* 41 (1978) 958.

[27] M. Mostoller and U. Landmann, *Phys. Rev*. B 20 (1979) 1755.

[28] M. Wutting, C. Oshima, T. Aizawa, R. Souda, S. Otami and Y. Ishizawa, *Surf. Sci.* 193 (1988) 180.

[29] L. Van Hove, *Phys. Rev.* 89 (1953) 1189.

[30] C. Kittel, *Introduction to solid state physics*, 8th ed., (Wiley, 2005).

[31] W. Kress, F. W. De Wette (Eds), *Surface Phonons*, (Springer-Verlag, Berlin, 1991).

[32] M. S. Rabia, *Physica E* 42 (2010) 307-1318.